

Collapse of skyrmions in two-dimensional ferromagnets and antiferromagnets

Liufei Cai, Eugene M. Chudnovsky, and D. A. Garanin

Department of Physics, Lehman College, City University of New York, 250 Bedford Park Boulevard West, Bronx, New York 10468-1589, USA

(Received 21 April 2012; published 24 July 2012)

Collapse of a skyrmion due to the discreteness of a crystal lattice in isotropic two-dimensional ferromagnets and antiferromagnets has been studied analytically and by numerical solution of equations of motion for up to 2000×2000 classical spins on a square lattice coupled via Heisenberg exchange interaction. Excellent agreement between analytical and numerical results has been achieved. The lifetime of the skyrmion scales with its initial size λ_0 as $(\lambda_0/a)^5$ in ferromagnets and as $(\lambda_0/a)^{2.15}$ in antiferromagnets with a being the lattice parameter. This makes antiferromagnetic skyrmions significantly shorter lived than ferromagnetic skyrmions.

DOI: [10.1103/PhysRevB.86.024429](https://doi.org/10.1103/PhysRevB.86.024429)

PACS number(s): 75.10.Hk, 12.39.Dc, 74.72.-h, 75.50.Ee

Skyrmions^{1,2} are topologically stable configurations of a fixed-length three-component vector field $\mathbf{n}(\mathbf{r})$ in the coordinate space of two dimensions. Due to the constraint $\mathbf{n}^2 = 1$, the \mathbf{n} field has two independent components. This permits unique mappings of $\mathbf{n} = (n_x, n_y, n_z)$ onto $\mathbf{r} = (x, y)$, described by classes of homotopy.³ Each homotopy class corresponds to a nontrivial field configuration characterized by a conserved topological charge. The emergence of a conserved charge from a continuous field theory prompted numerous studies of skyrmions in problems of high-energy and condensed-matter physics.⁴ They include cosmology,⁵ Bose-Einstein condensates,⁶ quantum Hall effect,^{7,8} and anomalous Hall effect,⁹ liquid crystals.¹⁰

The interest in skyrmions in ordered spin systems received much attention soon after the discovery of high-temperature superconductivity in copper oxides^{11–17} and have been further explored recently.^{18–21} It is related to the fact that superconductivity in copper oxides occurs in doped CuO_2 layers that, when undoped, are square lattices of antiferromagnetically ordered spins. Initially, there was some hope that interaction of electrons and holes with skyrmions could play some role in Cooper pairing, but this was never successfully demonstrated. Some indirect evidence of skyrmions in the magnetoresistance of lanthanum copper oxide has been recently reported,²² but direct observation of skyrmions in $2d$ antiferromagnetic (AFM) lattices is still lacking.

In a continuous field model, such as, e.g., the nonlinear σ model,²³ the ground-state energy of the skyrmion does not depend on its size λ . This follows from the invariance of the model with respect to the scale transformation $\mathbf{r} \rightarrow k\mathbf{r}$, where k is an arbitrary constant. If the skyrmion lives on a lattice, however, the scale invariance becomes broken due to the presence of a lattice parameter a . Thus, the energy of the skyrmion depends on its size. This, in general, must lead to the collapse or expansion of the skyrmion, making it unstable. The nature of the exchange interaction on a lattice makes the skyrmion energy decrease with its size, which leads to skyrmion collapse. A number of authors looked for interactions that could stabilize skyrmions in $2d$ ferromagnets (FMs).^{24–26} It was argued that an anisotropic crystal field added to the isotropic exchange model may, in principle, dynamically stabilize the skyrmion. In reality, however, anisotropic interactions are of relativistic origin, whereas, the lattice effect that leads to the collapse of the

skyrmion is of the exchange origin and, thus, much greater. The same is true about magnetic dipole-dipole interactions. In ferromagnets, macroscopic skyrmions could, in principle, be a part of a stable domain structure. This, however, would not apply to microscopic skyrmions. In antiferromagnets, long-range dipole-dipole interactions are negligible, and they cannot stabilize skyrmions of any size. Therefore, it is important first to understand what is the mechanism of skyrmion collapse in a generic exchange model.

In this paper, we study the dynamics of skyrmions and the dependence of their collapse time t_c on their initial size in a $2d$ square lattice of classical spins coupled via Heisenberg FM or AFM exchange interaction. The accuracy of the continuous approximation increases with the size of the skyrmion λ . One should, therefore, expect that the lattice skyrmion becomes stable in the limit of $\lambda \rightarrow \infty$. We find that t_c of the AFM skyrmion scales as $t_c \propto (\lambda_0/a)^{2.15}$ with its initial size λ_0 . We compute the dynamics of the collapse using both the analytical field model for the Néel vector and a direct numerical calculation on lattices of up to 2000×2000 exchange-coupled spins. The two approaches show excellent agreement with each other. For a $2d$ ferromagnet, we obtain (up to logarithmic corrections) the $(\lambda_0/a)^5$ scaling of the lifetime. This makes skyrmions significantly shorter lived in a $2d$ AFM than in a $2d$ FM.

We begin with an antiferromagnet described by the Hamiltonian for the Néel vector \mathbf{L} ,²³

$$\mathcal{H}_0 = \frac{1}{2} JS^2 \int dx dy \left[\frac{1}{c^2} \dot{\mathbf{L}}^2 + (\nabla \mathbf{L})^2 \right]. \quad (1)$$

Here, \mathbf{L} is normalized as $\mathbf{L}^2 = 1$, $(\nabla \mathbf{L})^2 \equiv (\partial_x \mathbf{L})^2 + (\partial_y \mathbf{L})^2$, $JS^2 > 0$ is the exchange energy associated with the interaction of spins of length S , and c is the speed of AFM spin waves that equals $2\sqrt{2}Ja/\hbar$ in a square lattice. The term with $\dot{\mathbf{L}}^2$ can be understood as a kinetic energy responsible for the inertia of antiferromagnets.

The absolute minimum of the energy corresponds to the uniform AFM background $\mathbf{L} = \text{const}$. Nonuniform configurations of \mathbf{L} are characterized by the topological charge,

$$Q = \frac{1}{4\pi a^2} \int dx dy \mathbf{L} \cdot (\partial_x \mathbf{L} \times \partial_y \mathbf{L}), \quad (2)$$

that takes values $Q = 0, \pm 1, \pm 2, \dots$. Within, e.g., the homotopy class $Q = -1$, the minimum energy static configuration

is a skyrmion given by

$$\mathbf{L} = \left(\frac{2\lambda x}{r^2 + \lambda^2}, \frac{2\lambda y}{r^2 + \lambda^2}, \frac{r^2 - \lambda^2}{r^2 + \lambda^2} \right), \quad (3)$$

where $r^2 = x^2 + y^2$. Its energy $E = 4\pi JS^2$ is independent of λ .

Equation (1) can be derived from the Heisenberg exchange interaction between nearest-neighbor classical spins $|\mathbf{s}^A| = |\mathbf{s}^B| = 1$,

$$\mathcal{H} = S^2 \sum_{ij} J_{ij} \mathbf{s}_i^A \cdot \mathbf{s}_j^B = -\frac{S}{2} \sum_{i \in A} \mathbf{s}_i^A \cdot \mathbf{H}_i^A - \frac{S}{2} \sum_{j \in B} \mathbf{s}_j^B \cdot \mathbf{H}_j^B, \quad (4)$$

where A and B denote AFM sublattices and $\mathbf{H}_i^{A,B} = -\delta\mathcal{H}/\delta(S\mathbf{s}_i^{B,A}) = -S \sum_j J_{ij} \mathbf{s}_j^{B,A}$ are the effective fields acting on the spins. As spins in each sublattice rotate smoothly through space, one can expand the effective fields as

$$\mathbf{H}_i^A = -JS \left[4\mathbf{s}_i^B + a^2 \nabla^2 \mathbf{s}_i^B + \frac{a^4}{12} (\partial_x^4 + \partial_y^4) \mathbf{s}_i^B + \dots \right], \quad (5)$$

and similarly for \mathbf{H}_i^B . This allows one to go over to the continuum description in which there are two spin fields \mathbf{s}^A and \mathbf{s}^B . Switching to the magnetization $\mathbf{M} = (\mathbf{s}^A + \mathbf{s}^B)/2$ and the Néel vector $\mathbf{L} = (\mathbf{s}^A - \mathbf{s}^B)/2$, satisfying $\mathbf{M}^2 + \mathbf{L}^2 = 1$ and $\mathbf{M} \cdot \mathbf{L} = 0$ with the help of equation of motion $\hbar \dot{\mathbf{s}}^{A,B} = [\mathbf{s}^{A,B} \times \mathbf{H}^{A,B}]$, one obtains

$$\mathcal{H} = \mathcal{H}_0 - \frac{1}{24} JS^2 a^2 \int dx dy [(\partial_x^2 \mathbf{L})^2 + (\partial_y^2 \mathbf{L})^2], \quad (6)$$

which differs from Eq. (1) by the second term due to the discreteness of the lattice. If the size of the skyrmion λ is large compared to a , this term can be treated as a perturbation. Using the ‘‘rigid’’ skyrmion profile of Eq. (3), one obtains the energy due to this term,

$$\mathcal{E}_{\text{discr}} = -(2\pi JS^2/3)(a/\lambda)^2, \quad (7)$$

that violates the scale invariance of the skyrmion. Equation (7) can be interpreted as a potential energy responsible for the skyrmion collapse. During the collapse, it is transformed into the kinetic energy defined by the integral of $\dot{\mathbf{L}}^2 = 4r^2(r^2 + \lambda^2)^{-2} \dot{\lambda}^2$. With an account of energy conservation, Eq. (6) gives

$$\frac{3}{c^2} \left(\ln \frac{r_{\text{max}}^2 + \lambda^2}{\lambda^2} - \frac{r_{\text{max}}^2}{r_{\text{max}}^2 + \lambda^2} \right) \dot{\lambda}^2 = \left(\frac{a}{\lambda} \right)^2 - \left(\frac{a}{\lambda_0} \right)^2, \quad (8)$$

where λ_0 is the initial size of the skyrmion and r_{max} has been introduced because of the logarithmic divergence of the integral in the kinetic energy. The natural choice is $r_{\text{max}} = \lambda_0 + ct$, which describes a front of AFM spin waves propagating away from the collapsing skyrmion. This is confirmed by direct numerical calculations, see Fig. 4 below. The logarithmic terms with time dependent r_{max} require numerical integration of Eq. (8). The resulting collapse curves are shown in Fig. 1.

We now turn to the direct numerical solution of the dynamics of the skyrmion provided by the microscopic Hamiltonian (4). The dynamics is determined by the coupled equation of motion for spins $\hbar \dot{\mathbf{s}}_i = -[\mathbf{s}_i \times \delta\mathcal{H}/\delta(S\mathbf{s}_i)]$. We chose the initial state as a staggered skyrmion texture \mathbf{s}^{st} , given by Eq. (3) for the A sublattice and by the same

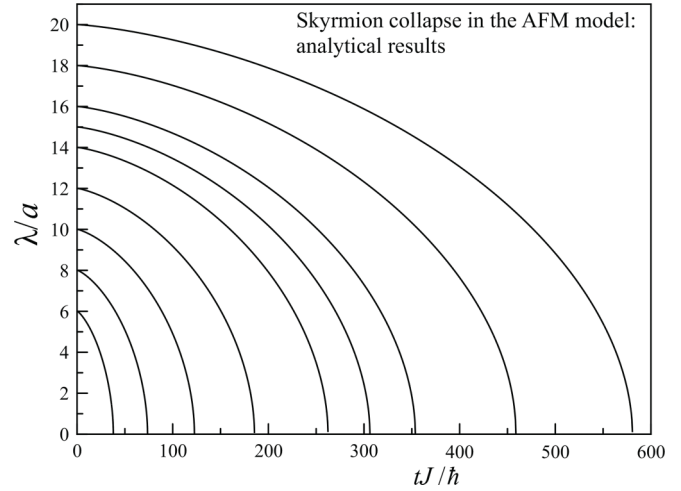


FIG. 1. Collapse of antiferromagnetic skyrmions as described by the numerical solution of Eq. (8).

formula but with a minus sign for the B sublattice. The size of the skyrmion numerically can be defined as $\lambda_m^2 = (m-1)(2^m \pi)^{-1} \sum_i (1 - s_{zi}^{\text{st}})^m$, where $m > 1$ is an integer. If one replaces the summation by integration over $dx dy/a^2$ and uses the skyrmion texture (3) for s_z^{st} , this formula becomes an identity $\lambda_m = \lambda$. The results presented below have been obtained with $m = 4$. Other options make little difference.

As the dynamics of the skyrmion is entirely due to small terms arising from the lattice discreteness, the time dependence is slow, and sufficient accuracy can be achieved even for a large time step of integration. Increasing the step is limited by stability rather than by required accuracy. The challenge of the numerical solution is the $1/r$ decay of the skyrmion profile that requires rather big lattice sizes even for moderate values of λ/a . Free or periodic boundary conditions introduce spurious λ -dependent energies that compete with the small energy due to the lattice discreteness, leading to the expansion of the skyrmion instead of collapse. To make boundary conditions more resembling an infinite lattice, we have included the missing outside neighbors of the boundary spins with the values approximated by the second-order extrapolation from the inside of the working region. Still, the lattice size has to be large: 1000×1000 for λ_0/a up to 16 and 2000×2000 for $\lambda_0/a = 18$ and 20. The program was implemented in Wolfram MATHEMATICA with a compiled vectorized fixed-step fourth-order Runge-Kutta routine. One AFM skyrmion-collapse event required about 1-h computer time.

The collapse of an AFM skyrmion with $\lambda_0/a = 15$ is shown in Fig. 2. Whereas, the skyrmion size λ decreases continuously, the topological invariant Q changes only during a short final stage of the collapse when the continuous approximation fails. Figure 3 shows skyrmion collapse curves for different values of λ_0/a . For $\lambda_0/a = 18$, the lattice size of 10^6 spins is too small, and computation with 4×10^6 spins is needed. For $\lambda_0/a = 16$, both these lattice sizes yield the same collapse curve. These results compare very well with the semianalytical results shown in Fig. 1. The collapse time can be fitted as $t_c \propto \lambda_0^{2.15}$ in this range of λ_0 . The considerable deviation from the square law can be traced back to the logarithmic term in Eq. (8). Figure 4 shows $|d\mathbf{L}/dt|$ in an antiferromagnetic skyrmion

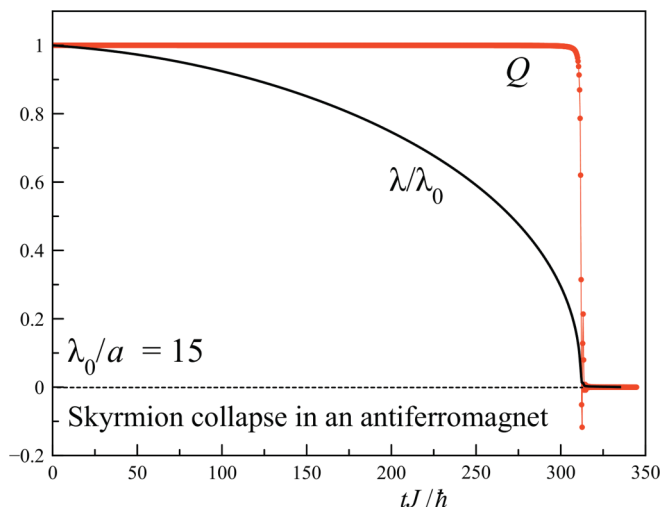


FIG. 2. (Color online) Skyrmion collapse in an antiferromagnet. Whereas, the skyrmion size λ decreases continuously, the topological charge Q decays only during a short final stage of the collapse.

at different times and the region of skyrmion motion where $|d\mathbf{L}/dt| > 0$ expands with the speed of antiferromagnetic spin waves c . The reason for this is that the lattice-discreteness terms that drive the skyrmion collapse are very short ranged, whereas, the skyrmion itself is long ranged. The action of the former is transferred to the whole skyrmion with a speed c in accordance with the causality. The front position can be estimated as $r_{\max} = \lambda_0 + ct$ as was argued after Eq. (8).

Along the same lines, we have numerically studied the dynamics of ferromagnetic skyrmions. It turns out to be much slower than the collapse of AFM skyrmions so that up to 1 day of computations is needed for one collapse event. Figure 5 shows time dependences of the size of FM skyrmions during the collapse. The collapse time scales as $t_c \propto \lambda_0^5$.

The λ_0^5 scaling of the collapse time of the FM skyrmion can be qualitatively understood as follows. The exchange interaction conserves the total spin of the system. The infinitesimal increase in the (negative) skyrmion spin in the

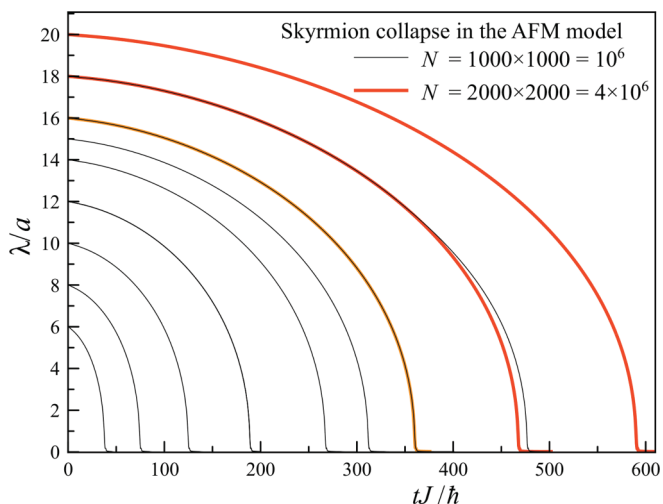


FIG. 3. (Color online) Skyrmion collapse in an antiferromagnet for different initial skyrmion sizes.

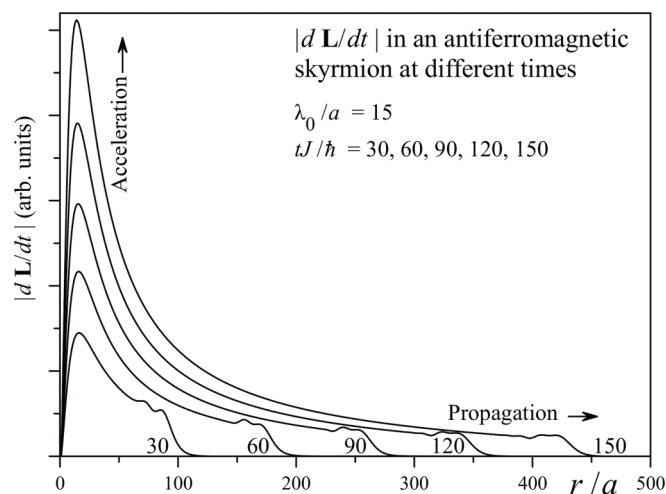


FIG. 4. The front propagating from the center of an antiferromagnetic skyrmion at the beginning of its collapse.

course of its collapse is

$$dS = S \int \frac{d^2r}{a^2} \frac{ds_z}{d\lambda} d\lambda = -8\pi S \frac{\lambda d\lambda}{a^2} \ln \frac{R}{\lambda}, \quad d\lambda > 0. \quad (9)$$

Here, we used s_z in the skyrmion form given by Eq. (3) and introduced the long-range cutoff R . Because of the conservation of the total spin, the increase in the skyrmion spin by dS generates dS magnons. Since, in this process, the spin is being carried by long distances, the skyrmion collapse is very slow. The average energy of emitted magnons can be estimated as $\hbar\omega \sim -\hbar\lambda/a$. This yields the emitted magnon power,

$$P = \hbar\omega \frac{dS}{dt} = 8\pi\hbar S \frac{\lambda\dot{\lambda}^2}{a^3} \ln \frac{R}{\lambda}. \quad (10)$$

On the other hand, the rate of change in the energy (7) due to discreteness of the lattice is $\dot{\mathcal{E}}_{\text{discr}} \propto \dot{\lambda}$. From the energy

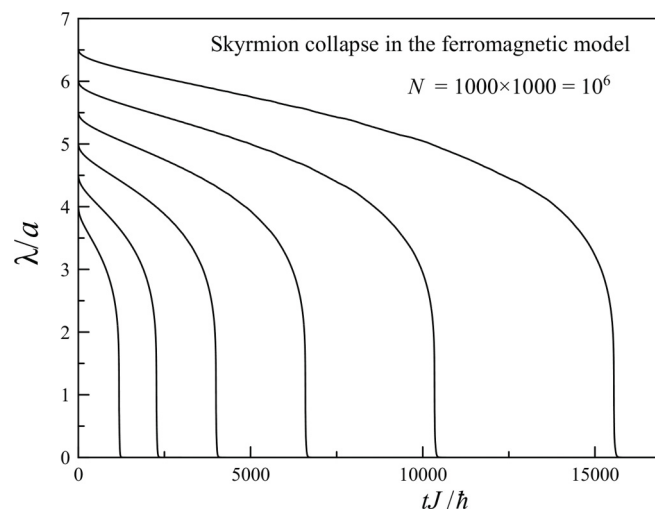


FIG. 5. Skyrmion collapse in a ferromagnet. The collapse time scales as $t_c \propto \lambda_0^5$.

conservation $\dot{\mathcal{E}}_{\text{discr}} + P = 0$, one obtains

$$\frac{d\lambda}{dt} = -\frac{JSa^5}{6\hbar} \frac{1}{\lambda^4 \ln(R/\lambda)}, \quad (11)$$

yielding the collapse time,

$$t_c = \frac{6\hbar}{5JS} \left(\frac{\lambda_0}{a}\right)^5 \ln\left(\frac{R}{\lambda_0}\right). \quad (12)$$

The condition $\hbar\omega \ll SJ$ for the energy of the magnons translates to $5(\lambda_0/a)^4 \ln(R/\lambda) \gg 1$, which is well satisfied during the collapse.

In conclusion, we have studied the collapse of skyrmions due to the discreteness of the lattice in generic models of isotropic $2d$ ferromagnets and antiferromagnets with Heisenberg exchange interaction. The results obtained within the continuous field model are in excellent agreement with the direct numerical calculation on lattices of up to 2000×2000 coupled spins. The collapse time of antiferromagnetic skyrmions, obtained by both methods, scales as $(\lambda_0/a)^{2.15}$. For ferromagnetic skyrmions, the numerical calculation gives the $(\lambda_0/a)^5$ scaling of the collapse time. It is explained by the emission of magnons. Thus, AFM skyrmions are much shorter lived than FM skyrmions. This can be understood in the following terms. The collapse of an AFM skyrmion occurs via transformation of its potential energy due to the discreteness of the lattice into the kinetic energy defined by $\dot{\mathbf{L}}^2$. The FM skyrmion does not possess such a kinetic energy so that its potential energy has to be dissipated into magnons, which is a much slower process. In the expression for t_c , the time constant in front of the power of the ratio λ_0/a is on the order of $\hbar/(JS)$.

For, e.g., $JS \sim 100$ K and $\lambda_0 \sim 10a$, this gives $t_c \sim 10$ ns for the lifetime of the skyrmion in a ferromagnet and $t_c \sim 10$ ps in an antiferromagnet. Skyrmions of sizes exceeding 1000 lattice spacings would be practically stable in a ferromagnet. In antiferromagnets, however, even macroscopic skyrmions would decay rather fast.

An interesting question is whether a skyrmion can be stabilized by the exchange interaction with an itinerant electron or a hole. If such an interaction is stronger than the exchange interaction between magnetic atoms in a $2d$ lattice, the electron polarizes the background, and the problem becomes one of the magnetic polaron. Only when the exchange interaction of the electron with the background is weak, can it be considered as a perturbation of the skyrmion problem. In the case of a ferromagnet, the energy of the electron in the uniform ferromagnetic background at infinity would always be lower than its energy in the vicinity of the skyrmion, thus, ruling out the stability of any bound state. For an antiferromagnet, the discreteness of the lattice generates a small uncompensated spin of the skyrmion. The electron can, in principle, couple to that spin by the exchange interaction. Our preliminary study shows, however, that this cannot prevent the skyrmion from collapsing. Full analysis of this problem will be presented elsewhere.

The authors thank O. Rübönkönig and D. Lichtblau of Wolfram Research for helping with the vectorization and compilation in Wolfram MATHEMATICA. This work has been supported by the Department of Energy through Grant No. DE-FG02-93ER45487.

¹T. H. R. Skyrme, *Proc. R. Soc. London, Ser. A* **247**, 260 (1958).

²A. A. Belavin and A. M. Polyakov, *Pis'ma Zh. Eksp. Teor. Fiz.* **22**, 503 (1975) [*JETP Lett.* **22**, 245 (1975)].

³A. M. Polyakov, *Gauge Fields and Strings* (Harwood Academic, Chur, Switzerland, 1987).

⁴*The Multifaceted Skyrmion*, edited by G. E. Brown and M. Rho (World Scientific, Singapore, 2010).

⁵R. Durrer, M. Kunz, and A. Melchiorri, *Phys. Rep.* **364**, 1 (2002).

⁶U. Al'Khawaja and H. T. C. Stoof, *Nature (London)* **411**, 918 (2001).

⁷S. L. Sondhi, A. Karlhede, S. A. Kivelson, and E. H. Rezayi, *Phys. Rev. B* **47**, 16419 (1993).

⁸M. Stone, *Phys. Rev. B* **53**, 16573 (1996).

⁹J. Ye, Y. B. Kim, A. J. Millis, B. I. Shraiman, P. Majumdar, and Z. Tesanovic, *Phys. Rev. Lett.* **83**, 3737 (1999).

¹⁰D. C. Wright and N. D. Mermin, *Rev. Mod. Phys.* **61**, 385 (1989).

¹¹P. B. Wiegmann, *Phys. Rev. Lett.* **60**, 821 (1988).

¹²B. I. Shraiman and E. D. Siggia, *Phys. Rev. Lett.* **61**, 467 (1988).

¹³X. G. Wen and A. Zee, *Phys. Rev. Lett.* **61**, 1025 (1988).

¹⁴S. Chakravarty, B. I. Halperin, and D. R. Nelson, *Phys. Rev. B* **39**, 2344 (1989).

¹⁵P. Voruganti and S. Doniach, *Phys. Rev. B* **41**, 9358 (1990).

¹⁶R. J. Gooding, *Phys. Rev. Lett.* **66**, 2266 (1991).

¹⁷S. Haas, F.-C. Zhang, F. Mila, and T. M. Rice, *Phys. Rev. Lett.* **77**, 3021 (1996).

¹⁸E. C. Marino and M. B. Silva Neto, *Phys. Rev. B* **64**, 092511 (2001).

¹⁹T. Morinari, *Phys. Rev. B* **65**, 064513 (2002).

²⁰T. Morinari, *Phys. Rev. B* **72**, 104502 (2005).

²¹Z. Nazario and D. I. Santiago, *Phys. Rev. Lett.* **97**, 197201 (2006).

²²I. Raicevic, D. Popovic, C. Panagopoulos, L. Benfatto, M. B. Silva Neto, E. S. Choi, and T. Sasagawa, *Phys. Rev. Lett.* **106**, 227206 (2011).

²³F. D. M. Haldane, *Phys. Rev. Lett.* **61**, 1029 (1988).

²⁴A. Abanov and V. L. Pokrovsky, *Phys. Rev. B* **58**, R8889 (1998).

²⁵B. A. Ivanov, A. Y. Merkulov, V. A. Stephanovich, and C. E. Zaspel, *Phys. Rev. B* **74**, 224422 (2006).

²⁶E. G. Galkina, E. V. Kirichenko, B. A. Ivanov, and V. A. Stephanovich, *Phys. Rev. B* **79**, 134439 (2009).